

# Superconducting phase coherence in the presence of a pseudogap: Relation to specific heat, tunneling, and vortex core spectroscopies

Qijin Chen\* and K. Levin

*James Franck Institute, University of Chicago, Chicago, Illinois 60637*

Ioan Kosztin

*Beckman Institute and Department of Physics, University of Illinois, Urbana, Illinois 61801*

(Received 28 September 2000; published 23 April 2001)

In this paper we demonstrate how, using a natural generalization of BCS theory, superconducting phase coherence manifests itself in phase-insensitive measurements—when there is a smooth evolution of the excitation gap  $\Delta$  from above to below  $T_c$ . In this context, we address the underdoped cuprates. Our premise is that just as Fermi-liquid theory fails above  $T_c$ , BCS theory fails below. The order parameter  $\Delta_{sc}$  is different from the excitation gap  $\Delta$ . Equivalently there is a (pseudo)gap in the excitation spectrum above  $T_c$  which is also present in the underlying normal state of the superconducting phase. A central emphasis of our paper is that the latter gap is most directly inferred from specific heat and vortex core experiments. At the same time there are indications that fermionic quasiparticles exist below  $T_c$  so that many features of BCS theory are clearly present. A natural reconciliation of these observations is to modify BCS theory slightly without abandoning it altogether. Here we review such a modification based on a BCS-like ground-state wave function. A central parameter of our extended BCS theory is  $\Delta^2 - \Delta_{sc}^2$  which is a measure of the number of bosonic pair excitations which have a nonzero net momentum. These bosons are present in addition to the usual fermionic quasiparticles. Applying this theory we find that the Bose condensation of Cooper pairs, which is reflected in  $\Delta_{sc}$ , leads to sharp peaks in the spectral function once  $T \leq T_c$ . These are manifested in angle-resolved photoemission spectra as well as in specific heat jumps, which become more like the behavior in a  $\lambda$  transition as the pseudogap develops. We end with a discussion of tunneling experiments and condensation energy issues. The comparison between theoretical and experimental plots of  $C_v$ , tunneling, vortex core spectroscopy measurements is good.

DOI: 10.1103/PhysRevB.63.184519

PACS number(s): 74.20.Fg, 74.25.Bt, 74.25.Fy

## I. INTRODUCTION

In the underdoped regime of high-temperature superconductors it is now clear that Fermi-liquid theory fails and the “smoking gun” for this failure is a (pseudo)gap in the fermionic excitation spectrum above  $T_c$ . Many would argue<sup>1,2</sup> that this failure is evidence for spin-charge separation. However, the fact that the excitation gap evolves smoothly into its counterpart in the superconducting phase may also be interpreted as evidence for “preformed pairs.” In this way superconducting pairing correlations are responsible for the breakdown of the Fermi liquid state. This picture appears rather natural in view of the notably short coherence length  $\xi$  in these materials, which leads to a breakdown of the strict mean-field theory of BCS. Within this short  $\xi$  scheme, one considers that pairs form at temperature  $T^*$  and Bose condense at lower temperature  $T_c$ . These are not true “preformed” or bound pairs but rather long-lived<sup>3-5</sup> pair states. Many have argued for this viewpoint from experimentalists<sup>6-10</sup> to theorists.<sup>11,12</sup>

Our contribution<sup>13-17</sup> to this body of work has been to show how to microscopically implement this preformed pair approach at all temperatures  $T \leq T_c$ , by deriving an extension of BCS theory, based on the ground state of Leggett.<sup>18</sup> We have also addressed<sup>3-5</sup> the behavior above  $T_c$ . In this extended BCS approach, the fermionic excitation gap  $\Delta$  [which evolves smoothly from above to below  $T_c$  (Refs. 19

and 20)] and the mean-field order parameter  $\Delta_{sc}$  (which is nonvanishing below  $T_c$ ) are not necessarily the same at any nonzero temperature; this is a reflection of the distinction between  $T^*$  and  $T_c$ . Since  $\Delta \neq \Delta_{sc}$ , we say that there are pseudogap effects below  $T_c$ . *The normal state underlying the superconducting phase is not a Fermi liquid.* The excitations of the system can be viewed as a “soup” of fermions and pairs of fermions (bosons). The latter are very long lived at and below  $T_c$  in the long-wavelength limit; their number is associated with the difference  $\Delta^2 - \Delta_{sc}^2$ .

This background sets the stage for the important questions which we address in this paper. What are the signatures of  $T_c$ , in thermodynamical quantities such as the specific heat  $C_v$ , given the smooth evolution of the excitation gap? How do we understand the abrupt appearance of long-lived, fermionic “quasiparticles” below  $T_c$  and their implications for the electronic spectral function  $A(\mathbf{k}, \omega)$ ? If the superconducting state is not Fermi-liquid based, then how does one extrapolate the “normal state” below  $T_c$  in order to deduce such thermodynamical properties as the condensation energy?

One of the central observations underlying this paper is the fact that there are two distinct experiments which provide seemingly similar information about the extrapolated normal state, i.e., that this  $T \leq T_c$  state contains an excitation gap. These are scanning tunneling microscopy (STM) data in a vortex core<sup>8,21</sup> as well as specific heat measurements.<sup>22</sup> Ren-

ner and co-workers<sup>8</sup> have argued that their vortex experiments “show either the presence of important superconducting fluctuations or pre-formed pairs.” Loram and co-workers<sup>22–24</sup> have analyzed their specific heat data to show that a thermodynamically consistent picture of  $C_v$  reflects a gap in the ( $T \leq T_c$ ) “normal”-state spectrum, not directly related to the condensate. This would, they argue, include the possibility of preformed pairs that retained their structure below  $T_c$ , as in <sup>4</sup>He, and whose binding energy does not contribute to the condensation energy. Alternative explanations for the vortex core experiments have been advanced by Franz and Millis<sup>25</sup> and, more recently, by Franz and Tesanovic<sup>26</sup> and by Lee and Wen.<sup>27</sup>

This “preformed pair” picture, which is essentially a mean-field-based approach, should be contrasted with the phase fluctuation picture of Emery and Kivelson<sup>28</sup> which has been implemented by Franz and Millis<sup>25</sup> to address photoemission and tunneling spectroscopies. In the present case the normal-state excitations represent a “soup” of fermions and bosons, whereas in the approach of Ref. 25 the system is thought to consist of a soup of fluctuating vortices. It is widely believed that, at least below  $T_c$ , fermionic quasiparticles are present so that the phase fluctuation picture will eventually need to accommodate their contributions. Loram *et al.*<sup>24</sup> have, moreover, argued that phase fluctuations are not consistent with the behavior of  $C_v$ , which they observe.

The results which we obtain in this paper show that upon entering the superconducting phase, the onset of the coherent condensate, characterized by  $\Delta_{sc}$ , leads to a sharpening of the peaks in the electronic spectral function, which will be directly reflected in angle-resolved photoemission spectroscopy (ARPES) studies where its effects are quite dramatic, as well as in tunneling.<sup>29</sup> ARPES measurements support such a peak sharpening, and it has been recently claimed,<sup>30</sup> as is consistent with the theme of this paper, that the observed sharpening at  $T_c$  (rather than at  $T^*$ ) is difficult to understand within strict BCS theory.

Indeed, BCS theory can and should be generalized, and in its more general form, this peak sharpening in conjunction with the temperature dependence of the excitation gap is also responsible for a specific heat jump. The latter is, thus, quite generally, associated with the onset of off-diagonal long-range order. When this general picture is applied to the cuprates we find that in the overdoped regime, this jump (in  $C_v$ ) can be quantified in terms of the temperature dependence of the excitation gap  $\Delta$  [as in the traditional BCS case; see Eq. (18) below]. This is in contrast to the underdoped regime, where the order parameter and excitation gap are distinct and where the excitation gap is smooth across  $T_c$ . Here the jump (associated only with  $\Delta_{sc}$ ) becomes smaller towards underdoping, where the pseudogap is more prominent. Moreover, the shape of the  $C_v$  versus  $T$  curve is more like the  $\lambda$  transition of Bose-Einstein condensation (BEC). All of these features seem to be consistent with experiment.<sup>24,6</sup>

An important second theme of this paper is an analysis of the extrapolated normal state below  $T_c$ . We argue here that the superconductivity is non-Fermi-liquid based and that this has important implications for condensation energy esti-

mates. Moreover, the non-Fermi-liquid characteristics of the extrapolated normal state (which underlies the superconducting phase) should help provide constraints on the long-standing controversy<sup>2</sup> of Fermi-liquid breakdown in the normal state. Indeed, spin-charge separation scenarios<sup>27,26</sup> might be distinguishable from alternatives such as the present one or that of Ref.25 by studies *below*  $T_c$ . This provides a major impetus for the present work.

## II. THEORETICAL FRAMEWORK

Our work begins with the ground-state wave function of BCS as generalized by Leggett,<sup>18</sup>

$$\Psi_0 = \Pi_{\mathbf{k}} (u_{\mathbf{k}} + v_{\mathbf{k}} c_{\mathbf{k}\uparrow}^\dagger c_{-\mathbf{k}\downarrow}^\dagger) |0\rangle, \quad (1)$$

which describes the continuous evolution between a BCS system, having weak coupling  $g$  and large  $\xi$ , towards a BEC system with large  $g$  and small  $\xi$ . Here  $u_{\mathbf{k}}, v_{\mathbf{k}}$ , which are defined as in BCS theory, are self-consistently determined in conjunction with the number constraint. *The central approximation of this paper is the choice of this ground-state wave function.* The essence of our previous contributions<sup>13,16,17</sup> has been a characterization of the excitations of  $\Psi_0$  and their experimental signatures (for all  $T \leq T_c$ ). New thermodynamical effects stemming from bosonic degrees of freedom must necessarily enter, as one crosses out of the BCS regime, towards Bose-Einstein condensation.

As in BCS theory, we presume that there exists some attractive interaction between fermions of unspecified origin which is written as  $V_{\mathbf{k},\mathbf{k}'} = g \varphi_{\mathbf{k}} \varphi_{\mathbf{k}'}$ , where  $g < 0$ ; here,  $\varphi_{\mathbf{k}} = 1$  and  $(\cos k_x - \cos k_y)$  for  $s$ - and  $d$ -wave pairing, respectively. The fermions are assumed to have dispersion,  $\epsilon_{\mathbf{k}} = 2t_{\parallel}(2 - \cos k_x - \cos k_y) + 2t_{\perp}(1 - \cos k_{\perp}) - \mu$ , measured with respect to the fermionic chemical potential  $\mu$ . Here  $t_{\parallel}$  and  $t_{\perp}$  are the in-plane and out-of-plane hopping integrals, respectively. In a quasi-two-dimensional (quasi-2D) system,  $t_{\perp} \ll t_{\parallel}$ . For brevity, we use a four-momentum notation  $K \equiv (\mathbf{k}, i\omega)$ ,  $\Sigma_K \equiv T \Sigma_{\mathbf{k},\omega}$ , etc., and suppress  $\varphi_{\mathbf{k}}$  until the final equations.

We now make a number of important observations about BCS theory. BCS theory involves a special form for the pair susceptibility  $\chi(Q) = \Sigma_K G(K) G_0(Q-K)$ , where the Green's function  $G$  satisfies  $G^{-1} = G_0^{-1} + \Sigma$ , with  $\Sigma(K) = -\Delta_{sc}^2 G_0(-K)$ . In this notation, the gap equation is

$$1 + g\chi(0) = 0, \quad T \leq T_c. \quad (2)$$

As was first observed by Kadanoff and Martin,<sup>31</sup> this BCS gap equation can be rederived by truncating the equations of motion so that only the one- ( $G$ ) and two-particle ( $T$ ) propagators appeared. Here  $G$  depends on  $\Sigma$  which in turn depends on  $T$ . In general  $T$  has two additive contributions,<sup>13</sup> from the condensate (sc) and the noncondensed (pg) pairs. Similarly the associated self-energy<sup>31</sup>

$$\Sigma(K) = \sum_Q T(Q) G_0(Q-K) \quad (3)$$

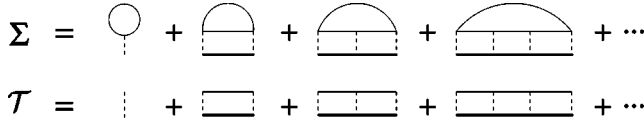


FIG. 1. Diagrammatic representation of the self-energy  $\Sigma$  and  $T$  matrix  $\mathcal{T}$ , as shown in Eq. (3). The thin and thick lines denote bare and full Green's functions, respectively.

can be decomposed into  $\Sigma_{pg}(K) + \Sigma_{sc}(K)$ . The two contributions in  $\Sigma$  come, respectively, from the condensate,  $\mathcal{T}_{sc}(Q) = -\Delta_{sc}^2 \delta(Q)/T$ , and from the  $Q \neq 0$  pairs, with  $\mathcal{T}_{pg}(Q) = g/[1 + g\chi(Q)]$ .

More generally, at larger  $g$ , the above equations hold but we now include feedback into Eq. (2) from the finite-momentum pairs, via  $\Sigma_{pg}(K) = \Sigma_Q \mathcal{T}_{pg}(Q) G_0(Q-K) \approx G_0(-K) \Sigma_Q \mathcal{T}_{pg}(Q) \equiv -\Delta_{pg}^2 G_0(-K)$ , which defines a pseudogap parameter  $\Delta_{pg}$ . This self-energy and the associated  $T$  matrix can be diagrammatically represented by Fig. 1.<sup>32</sup> This last approximation is valid only because [through Eq. (2)]  $\mathcal{T}_{pg}$  diverges as  $Q \rightarrow 0$ . A more complete discussion of the validity of this approximation, based on numerical studies, is given in Ref. 4. This body of work addresses the behavior when  $T_c$  is approached from above. Only at  $T_c$  can this approximation be made with any confidence, since otherwise the  $T$  matrix is not sufficiently peaked at small frequencies and wave vectors; this is equivalent to the statement that the temperature-dependent coherence length is not sufficiently long. Similar observations have been made elsewhere in the literature.<sup>33</sup> However, at all temperatures (at and below  $T_c$ , the gap equation or, alternatively, the generalized Thouless criterion of Eq. (2) helps to establish this important approximation. For the purposes of computing the gap parameters as a function of temperature ( $\Delta$  and  $\Delta_{sc}$ ), as well as  $T_c$ , we may use the approximation that  $\Sigma_{pg}(K)$  has a BCS-like form, as does, then, the total self-energy  $\Sigma(K) = -\Delta^2 G_0(-K)$ , where

$$\Delta^2 = \Delta_{sc}^2 + \Delta_{pg}^2. \quad (4)$$

For the physically relevant regime of moderate  $g$ , we have found, after detailed numerical calculations,<sup>15,16</sup> that  $\mathcal{T}_{pg}$  may be approximated as

$$\mathcal{T}_{pg}^{-1}(\mathbf{q}, \Omega) = a_0(\Omega - \Omega_{\mathbf{q}} + \mu_{pair} + i\Gamma_{\mathbf{q}}), \quad (5)$$

where the pair dispersion  $\Omega_{\mathbf{q}} = q^2/2M_{pair}$  and the effective pair chemical potential  $\mu_{pair} = 0$  for  $T \leq T_c$ . The effective pair mass  $M_{pair}$  and the coefficient  $a_0$  are determined via a Taylor expansion<sup>17</sup> of  $\mathcal{T}_{pg}^{-1}$ . Moreover,  $\Gamma_{\mathbf{q}} \rightarrow 0$ , as  $\mathbf{q} \rightarrow 0$ . As a consequence we have

$$\Delta_{pg}^2 = -\sum_Q \mathcal{T}_{pg}(Q) = \frac{1}{a_0} \sum_{\mathbf{q} \neq 0} b(\Omega_{\mathbf{q}}). \quad (6)$$

We now rewrite Eq. (2), along with the fermion number constraint, as

$$1 + g \sum_{\mathbf{k}} \frac{1 - 2f(E_{\mathbf{k}})}{2E_{\mathbf{k}}} \varphi_{\mathbf{k}}^2 = 0, \quad (7)$$

$$\sum_{\mathbf{k}} \left[ 1 - \frac{\epsilon_{\mathbf{k}}}{E_{\mathbf{k}}} + \frac{2\epsilon_{\mathbf{k}}}{E_{\mathbf{k}}} f(E_{\mathbf{k}}) \right] = n. \quad (8)$$

Here  $f(x)$  and  $b(x)$  are the Fermi and Bose functions and  $E_{\mathbf{k}} = \sqrt{\epsilon_{\mathbf{k}}^2 + \Delta^2 \varphi_{\mathbf{k}}^2}$  is the quasiparticle dispersion.

Before leaving this section, it is useful to recapitulate some key points of the above analysis. (i) The pair susceptibility  $\chi(Q)$  which we use throughout involves one bare and one dressed Green's function. This “ $GG_0$ ” scheme owes its origin to BCS theory, where this form for  $\chi$  leads to the BCS gap equation, rewritten as Eq. (2). Since we require that the present approach yield BCS theory at weak  $g$ , it is natural to introduce this form for our more general purposes.<sup>32</sup> (ii) Said alternatively, we can see that in weak coupling and at  $Q = 0$ , the integrand in  $\chi$  is proportional to the usual Gor'kov  $F$  function which is fundamental to BCS theory. Here the coefficient of proportionality is  $\Delta_{sc} = \Delta$ . (iii) It should be evident that, at stronger coupling, where these two energy gap parameters become distinct, it is not appropriate to introduce this anomalous form for the Green's function, since it is not clear whether in any given instance one should use the excitation gap  $\Delta$  or the order parameter  $\Delta_{sc}$ . By the same token, on general grounds, below  $T_c$  it is not sensible to use anomalous Green's functions in the pair susceptibility or in the self-energy. Rather their effects are accommodated via the introduction of the pair susceptibility in the “ $GG_0$ ” form. In the present approach it is the singular term in the  $T$  matrix,  $\mathcal{T}_{sc}$  (rather than the Gor'kov  $F$  function), which introduces the anomalous self-energy ( $\Sigma_{sc}$ ) into the formalism.

Finally, it should be stressed that Eqs. (6)–(8) represent the central equations of our theory below  $T_c$ . They are consistent with BCS theory at small  $g$  and with the ground state  $\Psi_0$  at all  $g$ ; in both cases the right hand side of Eq. (6) is zero. The simplest physical interpretation of the present decoupling scheme is that it goes beyond the standard BCS mean-field treatment of single particles (which also acquire a self-energy from finite  $\mathbf{q}$  pairs), but it *treats the pairs at a self-consistent mean-field level*.

### III. SPECTRAL FUNCTIONS, DENSITIES OF STATES, AND SPECIFIC HEAT

Experimentally, it has been established from specific heat measurements in the cuprates that there is a step discontinuity or a maximum at  $T_c$ , depending on the doping level.<sup>23,24</sup> It is clear that one cannot explain these experiments using the standard picture of BCS theory, in which the specific heat jump at  $T_c$  results from the opening of the excitation gap. We now address these experiments. In Sec. II, we used an approximate form for the pseudogap self-energy  $\Sigma_{pg}$  [see the derivation of Eq. (4)], in order to simplify the calculations. Under this approximation,  $\Sigma_{pg}$  has a BCS-like character, so that the spectral function is given by two  $\delta$  functions at  $\pm E_{\mathbf{k}}$ . These approximations were justified in the context of the applications considered thus far.<sup>13–17</sup>

However, in order to study quantities which rely on details of the density of states, we will, in the remainder of this paper, relax this simplifying approximation and allow for lifetime effects in  $\Sigma_{pg}$ . This more realistic form for  $\Sigma_{pg}$

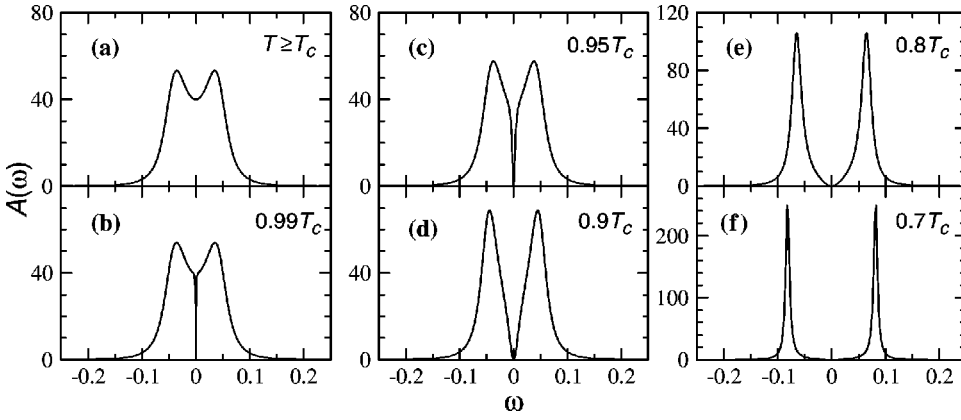


FIG. 2. Behavior of the coherent contribution to the spectral function at various  $T$ , for wave vectors away from the nodes.

incorporates a finite broadening  $\gamma$  due to the incoherent nature of the finite center-of-mass momentum pair excitations. In this way we distinguish this contribution from that of the condensate. To make numerical calculations tractable,<sup>4,5</sup> we do not solve for the broadening  $\gamma$  and excitation gap  $\Delta$  self-consistently. This would involve an iterative solution of the complex set of three coupled equations for  $G$  and  $\mathcal{T}$ ; rather we take  $\Delta$  below  $T_c$  from Eqs. (6)–(8), and use our estimates<sup>4,5</sup> of  $T^*$  to determine where pseudogap effects are essentially negligible. More importantly, we treat the broadening as a phenomenological parameter, with one adjustable coefficient, chosen to optimize fits to tunneling experiments. Our results, throughout this paper, are not particularly sensitive to the detailed form of  $\gamma$  (which will depend on doping concentration  $x$  and  $T$ ),<sup>34</sup> but it is essential that  $\gamma$  be nonzero and appreciable when compared with  $T$ . In this same spirit, we take  $T_c$  and the chemical potential  $\mu$  from our leading order calculations (with  $\gamma=0$ ).

We turn now to the spectral function  $A(\mathbf{k}, \omega)$ . It follows from our microscopic scheme that slightly above<sup>4,5</sup>  $T_c$  and for all  $T \leq T_c$ ,<sup>13</sup> the self-energy associated with the  $\mathbf{q} \neq 0$  pairs and that from the condensate or  $\mathbf{q} = 0$  pairs are given, respectively, by

$$\Sigma_{pg}(\mathbf{k}, \omega) = \frac{\Delta_{\mathbf{k}, pg}^2}{\omega + \epsilon_{\mathbf{k}} + i\gamma} - i\Sigma_0(\mathbf{k}, \omega) \quad (9)$$

and

$$\Sigma_{sc}(\mathbf{k}, \omega) = \frac{\Delta_{\mathbf{k}, sc}^2}{\omega + \epsilon_{\mathbf{k}}}, \quad (10)$$

where  $\Delta_{\mathbf{k}, pg} = \Delta_{pg} \varphi_{\mathbf{k}}$  and  $\Delta_{\mathbf{k}, sc} = \Delta_{sc} \varphi_{\mathbf{k}}$ . Here we have added to  $\Sigma_{pg}$  an additional piece  $\Sigma_0$  which is not accounted for by our (particle-particle) ladder diagrams. This leads to an ‘‘incoherent’’ background contribution which we will address later in the context of the cuprates. For the rest of the discussion in the next two sections we set  $\Sigma_0 = 0$  and, thereby, focus only on the superconducting and pseudogap terms.

The spectral function can readily be computed from  $\Sigma = \Sigma_{sc} + \Sigma_{pg}$ , as

$$A(\mathbf{k}, \omega) = -2 \operatorname{Im} G(\mathbf{k}, \omega + i0), \quad (11)$$

which satisfies the sum rule  $\int_{-\infty}^{\infty} (d\omega/2\pi) A(\mathbf{k}, \omega) = 1$ . We thus obtain a relatively simple expression for  $A(\mathbf{k}, \omega)$  which applies below and above  $T_c$ , respectively,

$$A(\mathbf{k}, \omega) = \frac{2\Delta_{\mathbf{k}, pg}^2 \gamma (\omega + \epsilon_{\mathbf{k}})^2}{(\omega + \epsilon_{\mathbf{k}})^2 (\omega^2 - E_{\mathbf{k}}^2)^2 + \gamma^2 (\omega^2 - \epsilon_{\mathbf{k}}^2 - \Delta_{\mathbf{k}, sc}^2)^2}, \quad (12a)$$

$$A(\mathbf{k}, \omega) = \frac{2\Delta_{\mathbf{k}}^2 \gamma}{(\omega^2 - E_{\mathbf{k}}^2)^2 + \gamma^2 (\omega - \epsilon_{\mathbf{k}})^2}. \quad (12b)$$

From Eq. (12b), we see that the spectral function contains a zero at  $\omega = -\epsilon_{\mathbf{k}}$  below  $T_c$ , whereas it has no zero above  $T_c$ . This difference is responsible for the different thermodynamical behavior across  $T_c$ .

In Fig. 2, we plot the spectral function for  $\epsilon_{\mathbf{k}} = 0$  (on the Fermi surface) at different temperatures from slightly above  $T_c$  [Fig. 2(a)] to temperatures within the superconducting phase [Fig. 2(f)]. This figure is typical of situations in which there is a well-established pseudogap. The figure can be viewed as representative of both  $s$ - and  $d$ -wave order parameter symmetries. Hence the value of the wave vector  $\hat{k}$  is not particularly relevant, provided it is away from the nodal points in the  $d$ -wave case. For illustrative purposes, we take  $\hat{k}$  at the antinodes, with  $\gamma(T) = \Delta_{pg}(T_c)$  and  $\Delta_{pg}(T_c) = 0.05$  (in units of  $4t_{\parallel}$ ). In this way we ignore any  $T$  dependence in  $\gamma$  and, thus, single out the long-range order effects associated with  $\Delta_{sc}$ .

These figures give the first clear indications of the onset of ‘‘quasiparticle’’ coherence. Moreover, panel (a) helps to emphasize an important component of our physical picture: the superconductor is not in a Fermi-liquid state just above  $T_c$ , as can be seen by the non-Fermi-liquid form for the spectral function. Just below  $T_c$ , the dramatic dip at  $0.99T_c$  is a consequence of Bose condensation of  $\mathbf{q} = 0$  pairs. Here, a very small condensate contribution nevertheless leads to the depletion of the spectral weight at the Fermi level, as shown in Fig. 2(b). As the temperature continues to decrease and the superconducting gap increases, the two peaks in the spectral function become increasingly well separated, as plotted in Figs. 2(c)–2(f). Even at the relatively high temperatures corresponding to  $T/T_c \sim 0.7$ , the spectral peaks are quite

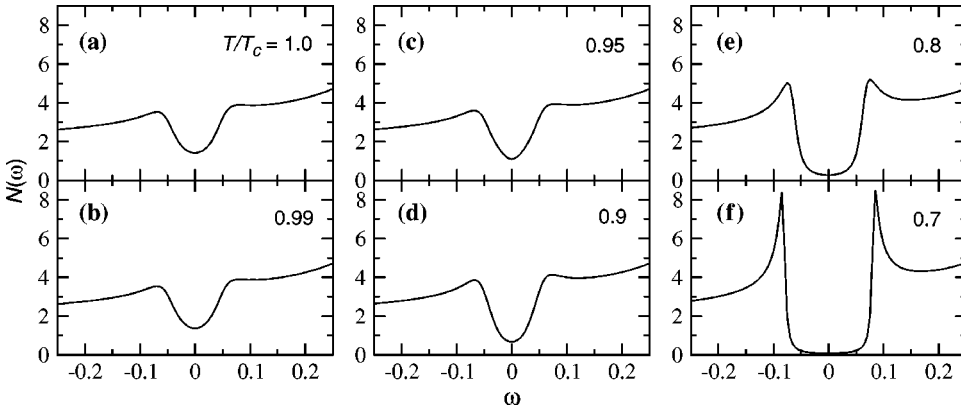


FIG. 3. Effects of superconducting long-range order on the behavior of the density of states as a function of temperature in a pseudogapped  $s$ -wave superconductor with  $n=0.5$ . Here we take the parameters to be the same as those used in Fig. 2. At  $T/T_c \sim 0.7$ , as shown in (f), the density of states is close to that of strict BCS theory.

sharp—only slightly broadened relative to their BCS counterparts (where the spectral function is composed of two  $\delta$  functions).

It should be stressed that lifetime effects via  $\gamma$  do not lead to significant peak broadening. This follows from the fact that the imaginary part of the pseudogap self-energy at the peak location  $E_{\mathbf{k}}$  is given by (for  $\epsilon_{\mathbf{k}}=0$ )

$$\gamma' = \gamma \frac{\Delta_{\mathbf{k},pg}^2}{(E_{\mathbf{k}} + |\epsilon_{\mathbf{k}}|)^2 + \gamma^2} = \gamma \frac{\Delta_{\mathbf{k},pg}^2}{\Delta_{\mathbf{k}}^2 + \gamma^2}. \quad (13)$$

Since Eq. (6) indicates that  $\Delta_{pg}$  vanishes as  $T \rightarrow 0$ , the effective peak width, determined by  $\gamma'$ , decreases with decreasing  $T$ . It can be seen that below  $T_c$ , the spectral function in Eq. (12b), is very different from that obtained using a simple broadened BCS form; there is no true gap for the latter, in contrast to the present case.

These spectral functions can be used to derive the density of states (per spin) as

$$N(\omega) = \sum_{\mathbf{k}} A(\mathbf{k}, \omega). \quad (14)$$

Moreover, it is expected that peak sharpening effects discussed above for the spectral function are also reflected in the density of states. For simplicity, we first consider the case of  $s$ -wave pairing. In Figs. 3(a)–3(f), the density of states is plotted for a quasi-2D  $s$ -wave superconductor, where the various energy gaps are taken to be the same as in Fig. 2. Because of contributions from states with  $\epsilon_{\mathbf{k}} \neq 0$ , the narrow dips in Figs. 2(b) and 2(c) do not show up here. However, as is evident, the density of states within the gap region decreases quickly, as the superconducting condensate develops.

The rapid decrease of the density of states with decreasing  $T$ , in the vicinity of  $T_c$ , will be reflected in the behavior of the specific heat  $C_v$  and, thereby, leads to the thermodynamical signature of the phase transition.  $C_v$  may be obtained from  $C_v = dE/dT$ , where the energy  $E$  is calculated via<sup>35</sup>

$$\begin{aligned} E &= 2T \sum_{\mathbf{k}, n} \frac{1}{2} (i\omega_n + \epsilon_{\mathbf{k}}^0 + \mu) G(\mathbf{k}, i\omega_n) \\ &= \sum_{\mathbf{k}} \int_{-\infty}^{\infty} \frac{d\omega}{2\pi} (\omega + \epsilon_{\mathbf{k}} + 2\mu) A(\mathbf{k}, \omega) f(\omega), \end{aligned} \quad (15)$$

where  $\epsilon_{\mathbf{k}}^0 = \epsilon_{\mathbf{k}} + \mu$  is the dispersion measured from the bottom of the band. It follows that

$$E = \int_{-\infty}^{\infty} \frac{d\omega}{2\pi} [(\omega + \mu)N(\omega) + K(\omega)] f(\omega), \quad (16)$$

where we have defined  $K(\omega) \equiv \sum_{\mathbf{k}} \epsilon_{\mathbf{k}}^0 A(\mathbf{k}, \omega)$ , which can be regarded as the contribution associated with the kinetic energy of the system. In this way, we obtain

$$\begin{aligned} C_v &= \int_{-\infty}^{\infty} \frac{d\omega}{2\pi} \left\{ \frac{\partial \mu}{\partial T} N(\omega) f(\omega) - [(\omega + \mu)N(\omega) \right. \\ &\quad \left. + K(\omega)] \frac{\omega}{T} f'(\omega) + \left[ (\omega + \mu) \frac{\partial N(\omega)}{\partial T} + \frac{\partial K(\omega)}{\partial T} \right] f(\omega) \right\}. \end{aligned} \quad (17)$$

The first two terms on the right hand side lead to a ‘‘normal-metal-like’’ contribution to  $C_v/T$  which is proportional to  $N(\omega)$  at low  $T$ . However, the third term arises because  $N(\omega)$  depends on  $T$ . In this case,  $C_v/T$  no longer reflects the density of states. It is this term that will give rise to the specific heat discontinuity at  $T_c$ .

In Fig. 4 we plot the temperature dependence of  $C_v$  in both (a) the weak-coupling BCS case and (b) the moderate-coupling pseudogap case with  $s$ -wave pairing. We choose, for definiteness, the broadening  $\gamma(T) = T$  for the second of these calculations. We also indicate in the insets the respective temperature-dependent excitation gaps, which have been assumed<sup>13,16</sup> in producing the figure.

In both cases shown in Fig. 4, the specific heat jump arises from a discontinuity in  $dN(\omega)/dT$ ,<sup>36</sup> associated with the onset of superconducting order. However, for the BCS case, this derivative can be associated with a discontinuity in the derivative of the excitation gap, via

$$\Delta C_v^{BCS} = -N(0) \frac{d\Delta^2}{dT}. \quad (18)$$

By contrast, in the pseudogap case, the gap  $\Delta$  and its derivative  $d\Delta/dT$  are presumed to be continuous across  $T_c$  as shown in the inset to Fig. 4(b) and in Fig. 5 below, so that Eq. (18) does not hold. Moreover, in this case, above but near  $T_c$ , the temperature dependence in the density of states is still important due to the presence of an excitation gap

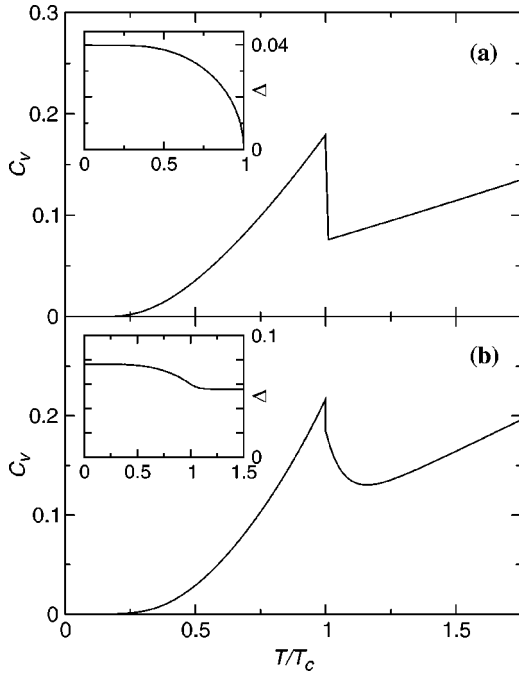


FIG. 4. Comparison of the temperature dependence of the specific heat in the (a) weak-coupling BCS case and (b) moderate-coupling pseudogap case. Shown here are quasi-2D  $s$ -wave results, at  $n=0.5$ ,  $-g/4t_{\parallel}=0.5$  and  $0.6$ , respectively. The  $T$  dependence of the gap is shown as insets.

above  $T_c$ . The latter leads to a decrease in  $dN(\omega)/dT$  which is then reflected<sup>37</sup> in a decrease in  $C_v$ , slightly above  $T_c$ . At higher  $T$ , well away from  $T_c$ , where  $dN(\omega)/dT$  tends gradually to zero,  $C_v$  is then controlled, as in a more typical “normal metal,” by  $N(\omega)$ . We see, then, that the approach to the “normal metal” value is sharp for the BCS case, but because of the nonzero pseudogap, it is more gradual for case (b). An important consequence of these effects, is that the shape of

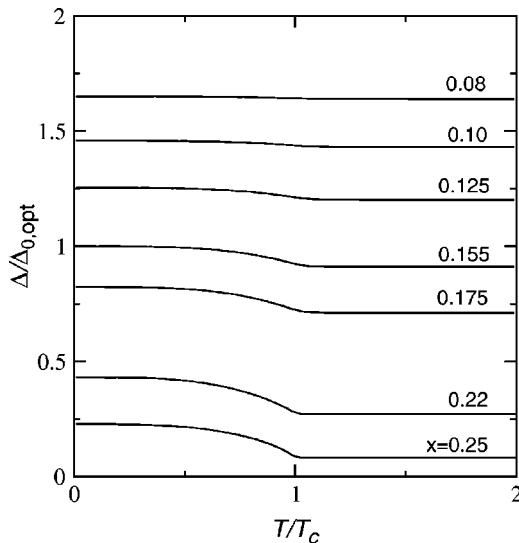


FIG. 5. Temperature dependence of the excitation gaps for various doping concentrations used for calculations in Fig. 7. Here  $\Delta_{0,opt}$  is the zero- $T$  gap at optimal doping  $x \approx 0.15$ .

the anomaly in  $C_v$  [shown in Fig. 4(b)] is more characteristic of a  $\lambda$ -like transition, although there is a precise step function discontinuity just at  $T_c$ .

#### IV. APPLICATION TO THE CUPRATES

The results obtained in Sec. III are generally valid for both  $s$ - and  $d$ -wave cases, and can be readily applied to the  $d$ -wave cuprates. In this section we test the physical picture and the results obtained above by studying the tunneling spectra and the specific heat behavior in the cuprates as a function of doping and of temperature. As in earlier work,<sup>16,17</sup> we introduce a hole concentration dependence of the electronic energy scales by imposing the Mott constraint that the in-plane hopping integral  $t_{\parallel}(x)=t_0x$ , so that the plasma frequency vanishes as  $x \rightarrow 0$ . As a result, the effective coupling strength  $-g/t_{\parallel}(x)$  increases as the Mott insulator phase is approached. Here we assume (for simplicity)  $g(x)=g$  and fit the one free parameter  $g/t_0$  to the phase diagram.<sup>16</sup>

In order to compare with tunneling spectra, we introduce a slightly more realistic band structure which includes a next-nearest-neighbor hopping term  $-2t'(1-\cos k_x \cos k_y)$  in the band dispersion  $\epsilon_{\mathbf{k}}$ , with  $t'/t_{\parallel} \approx 0.4$ . This parameter choice gives rise to the holelike Fermi surface shape seen in ARPES measurements for underdoped and optimally doped cuprates,<sup>38,39</sup> and places the van Hove singularity in a more correct position within the band.

Finally, we turn to the phenomenological parameter  $\gamma$  as well as to  $\Delta$ . We presume that  $\gamma$  changes from above to below  $T_c$  and in this way  $\Delta$  (which is directly coupled to  $\gamma$  via the set of coupled equations for  $G$  and  $T$ ) will have some, albeit small, structure in its temperature dependence at  $T_c$ , as seems to be the case experimentally. Our choice for the excitation gaps is shown in Fig. 5, and appears compatible with Figs. 8 and 9 in Ref. 22. As is consistent with scattering rate measurements in the literature,<sup>40,41</sup> we take  $\gamma \propto T^3$  below  $T_c$  and linear in  $T$  above  $T_c$ .<sup>42</sup> For the doping dependence, we assume that  $\gamma$  varies inversely with  $\Delta$ . This reflects the fact that when the gap is large, the available quasiparticle scattering decreases. With these reasonable assumptions, along with the continuity of  $\gamma$  at  $T_c$ , we obtain a simple form

$$\gamma = \begin{cases} aT^3/T_c\Delta & (T < T_c), \\ aTT_c/\Delta & (T > T_c). \end{cases} \quad (19)$$

Here, the coefficient  $a \leq 1$ . This corresponds to our single adjustable parameter.

##### A. Tunneling spectra

Tunneling experiments were among the first to provide information about the excitation gap—which measurements seem to be consistent with ARPES data.<sup>9</sup> For a given density of states  $N(\omega)$ , the quasiparticle tunneling current across a superconducting-insulator-normal (SIN) junction can be readily calculated,<sup>43</sup>

$$I_{SIN} = 2eN_0T_0^2 \int_{-\infty}^{\infty} \frac{d\omega}{2\pi} N(\omega) [f(\omega - eV) - f(\omega)], \quad (20)$$

where we have assumed a constant density of states,  $N_0$ , for the normal metal, and presumed that the tunneling matrix element  $T_0$  is isotropic. In reality, there may be some directional tunneling which will tend to accentuate the gap features, but we do not complicate our discussion here with these effects. At low  $T$ , one obtains

$$\left(\frac{dI}{dV}\right)_{SIN} \approx \frac{e^2N_0T_0^2}{\pi} N(eV) \quad (21)$$

so that the tunneling spectra and the density of states are equivalent, up to a multiplicative constant coefficient. At  $T$  comparable to  $T_c$ , however, the tunneling spectra reflect a more thermally broadened density of states.

In Fig. 6(a), we plot the SIN tunneling spectra, calculated for optimal doping ( $x \approx 0.15$ ) at temperatures varying from above to below  $T_c$ . The van Hove singularity introduces a broad maximum in the spectra at high temperatures, as seen for the top curve in Fig. 6(a). We see here that (even for this optimal sample), as observed experimentally,<sup>9</sup> the density of states contains (pseudo)gaplike features which lead to two peaks. This is visible for temperatures well above  $T_c$ . A similar plot is presented in Fig. 6(b), which shows at fixed low  $T = 0.2T_c$  how the spectrum evolves as a function of  $x$ . Both these plots appear in reasonable agreement with what is observed experimentally by Renner and co-workers<sup>44</sup> and by Miyakawa *et al.*<sup>45</sup> for  $\text{Bi}_2\text{Sr}_2\text{CaCu}_2\text{O}_{8+\delta}$  (Bi2212).

### B. Specific heat

There is a substantial amount of experimental data on the specific heat in the cuprates,<sup>24,6</sup> although systematic studies come primarily from one experimental group.<sup>24</sup> We compare our numerical results with these data by plotting our calculations for  $C_v/T$  in Figs. 7(a)–7(f), from over- to underdoped systems. As shown in these plots, the behavior of  $C_v$  is BCS-like in the overdoped regime. As the system passes from optimal doping towards underdoping, the behavior is more representative of a  $\lambda$ -like anomaly, as found in Fig. 4(b) for the  $s$ -wave case. All these trends seem to be qualitatively consistent with experimental data.<sup>23,24</sup> In the underdoped regime at high  $T$ , we find a maximum in  $C_v/T$ , near a temperature  $T^*$ , which may be associated with the onset of the pseudogap state [see, e.g., Fig. 8(c)]. Finally, in contrast to Fig. 4, at low  $T$ , the  $d$ -wave nodes lead to a larger quasi-particle specific heat, than for the  $s$ -wave case.

The experimentally observed  $\lambda$ -like anomaly of  $C_v$  at  $T_c$  has been interpreted previously as evidence for a Bose condensation description.<sup>6</sup> Here, in contrast, we see that within our generalized mean-field theory, this anomaly naturally arises from the temperature dependence of the fermionic excitation gap which has some structure at, but persists above,  $T_c$ , as shown in Fig. 5. Thus, this is a property of superconductors which have a well-established pseudogap. That the experimental data (which, except at extremely reduced hole concentrations) show a reasonably sharp ( $\lambda$ -like) structure at

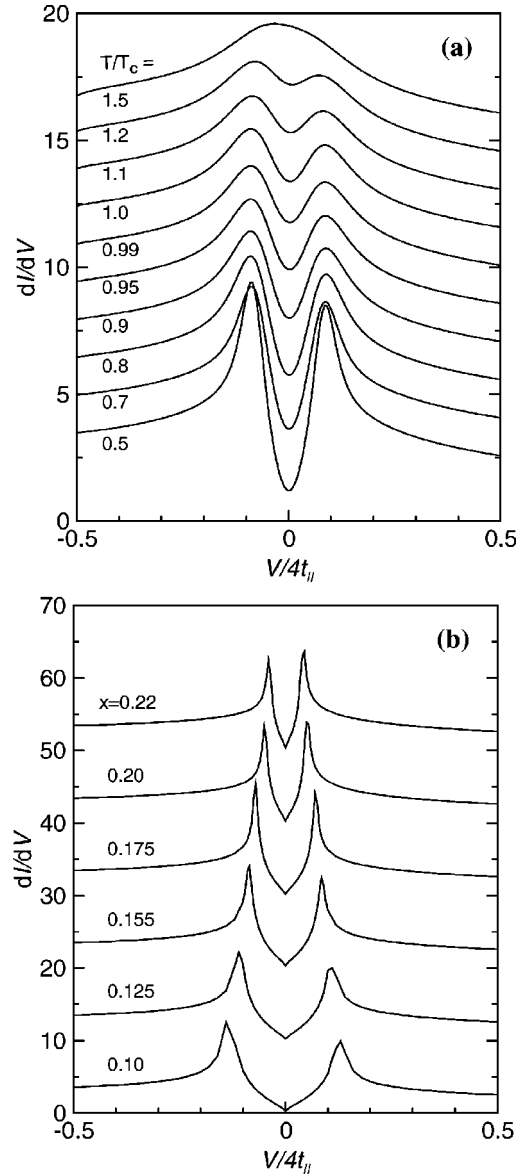


FIG. 6. (a) Temperature and (b) doping dependence of tunneling spectra across an SIN junction. Shown in (a) are the  $dI/dV$  characteristics calculated for optimal doping at various temperatures from above to below  $T_c$ . Shown in (b) are tunneling spectra at low  $T$  (at  $0.2T_c$ ) for various  $x$ . The units for  $dI/dV$  are  $e^2N_0T_0^2/4t_{\parallel}$ , where  $t_{\parallel}$  is evaluated at optimal doping. For clarity, the curves in (a) and (b) are vertically offset by 1.5 and 10, respectively.

$T_c$  seems to reinforce the general theme of this work—that corrections to BCS theory may be reasonably accounted for by an improved mean-field theory, rather than by, say, including order parameter fluctuation effects.

## V. LOW- $T$ EXTRAPOLATION OF THE PSEUDOGAPPED NORMAL STATE

### A. Non-Fermi-liquid-based superconductivity

The character of the extrapolated ( $T \leq T_c$ ) “normal state” is at the core of many topical issues in high- $T_c$  superconductivity. Understanding this state may shed light on the nature

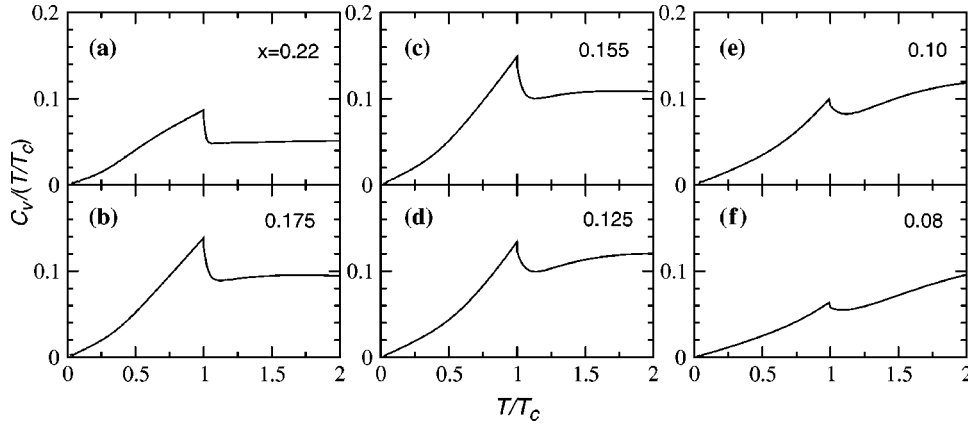


FIG. 7. Temperature dependence of the specific heat for various doping concentrations, calculated with  $a = 1/4$  in Eq. (19).

of Fermi-liquid breakdown above  $T_c$ . Moreover, the thermodynamics of this extrapolated phase provides a basis for estimates of the condensation energy. This is deduced<sup>24</sup> by integrating the difference between the entropy of the superconducting state and that of the extrapolated normal state with respect to  $T$ . This extrapolated normal state also appears as a component of the free energy functional of conventional Landau-Ginzburg theory. Indeed, considerable attention has been paid recently to condensation energy in the context of determining the pairing “mechanism” in high-temperature superconductors.<sup>46–48</sup> In this regard what is needed is the difference between the various “normal”- and superconducting-state polarizabilities (e.g., magnetic and electric) which are thought to be responsible for the pairing. It is important to stress that the “normal state” used in computing the polarizabilities should contain an excitation gap which is compatible with that found in the experimental data analysis<sup>24</sup> with which the microscopically deduced condensation energy is compared.

We have emphasized that within our physical picture there is an underlying (pseudo)gap in the normal state below  $T_c$ . A similar picture was independently deduced phenomenologically from specific heat and magnetic susceptibility measurements by Loram and co-workers<sup>22</sup> who arrived at equations like those of Sec. II [Eqs. (4) and (7)]. However, they did not impose a self-consistent condition on  $\Delta_{pg}$  as in Eq. (6). Rather the quantity  $\Delta_{pg}$  (which they call  $E_g$ ) is assumed to be  $T$  independent.

To expand on these issues we plot in Fig. 8 the calculated  $C_v/T$  and entropy  $S$  for (a) and (b) the BCS case, as compared with the counterparts obtained for the pseudogap superconductor in (c) and (d). The dotted lines represent the Fermi liquid, i.e., linear extrapolation (FL). Figures 8(a) and 8(b) reaffirm that this Fermi-liquid extrapolation is sensible for the BCS case— $C_v/T$  is a constant, and  $S$  is a straight line going through the origin. Panel (b) is useful in another respect: it shows how the entropy behaves as phase coherence is established. In general, the phase-coherent state has a lower entropy than the extrapolated normal state.

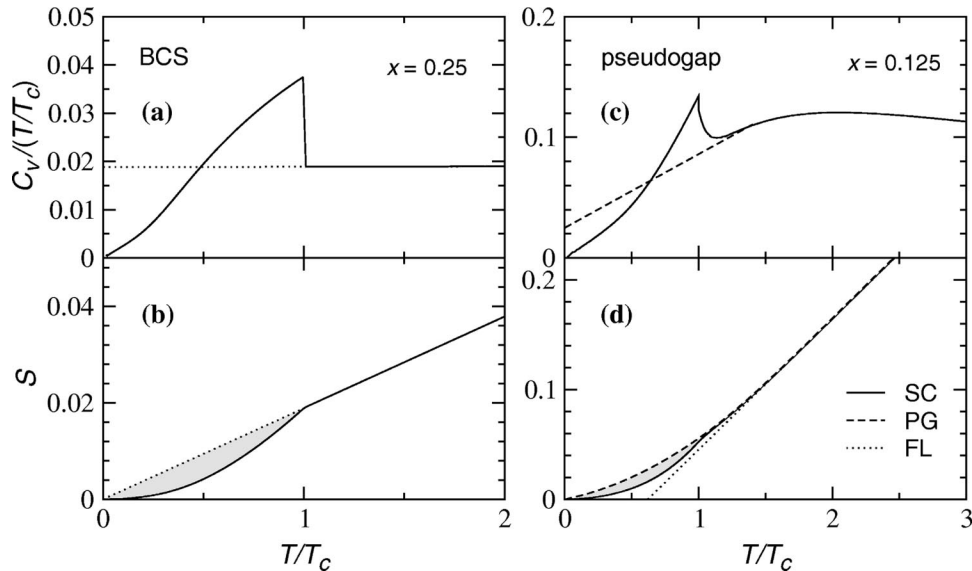


FIG. 8. Comparison of the extrapolated normal state below  $T_c$  in (a),(b) BCS and (c),(d) pseudogap superconductors. Shown are the extrapolations for  $C_v/T$  and the entropy  $S$  in the upper and lower panels, respectively. Here “SC,” “PG,” and “FL” denote superconducting state, extrapolated normal state with a pseudogap, and Fermi-liquid-based extrapolation, respectively. The shaded areas in (c) and (d) determine the condensation energy.



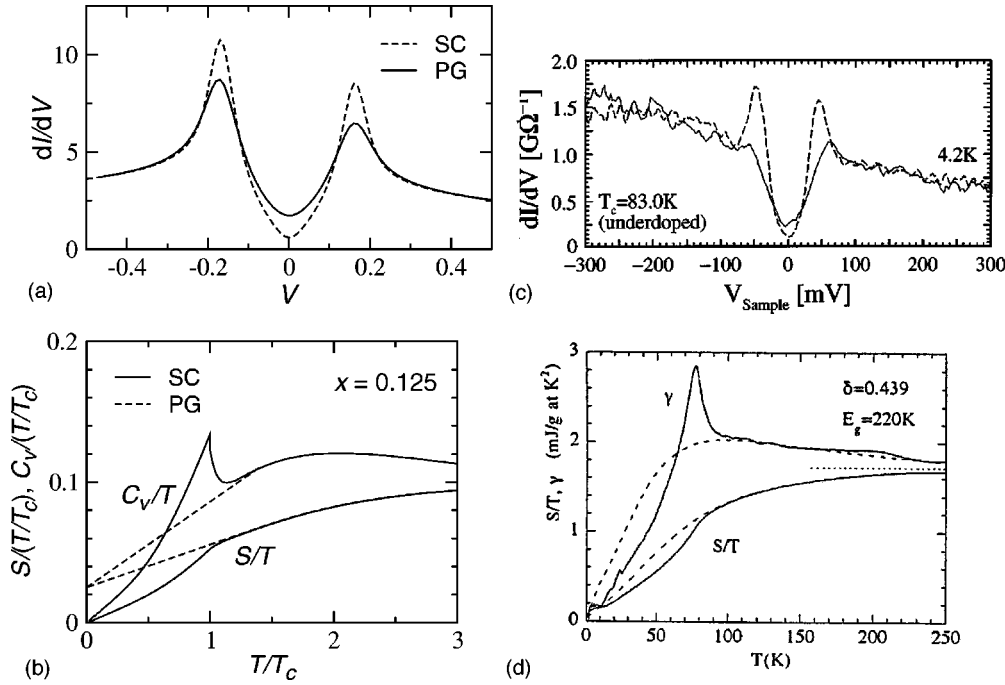


FIG. 9. Extrapolated normal-state (PG) and superconducting-state (SC) contributions to SIN tunneling and thermodynamics (left), as well as comparison with experiments (right) on tunneling for Bi2212 from Renner *et al.* (Ref. 8) and on specific heat for  $Y_{0.8}Ca_{0.2}Ba_2Cu_3O_{7-\delta}$  from Loram *et al.* (Ref. 24). The theoretical SIN curve is calculated for  $T = T_c/2$ , while the experimental curves are measured outside (dashed line) and inside (solid line) a vortex core.

In the underdoped regime, Loram and co-workers<sup>24</sup> have stressed that entropy measurements lead one to infer that an excitation gap occurs *above*  $T_c$ . We analyze our calculated form of the entropy in a similar fashion. In contrast to the BCS case, for a pseudogap superconductor, the Fermi-liquid extrapolation of  $S$  is unphysical, approaching a negative value at low  $T$ , as shown by the dotted line in Fig. 8(d). Here the solid and dotted lines separate around the temperature  $T^*$  which we find to be around  $1.5T_c$ . In order to obtain a thermodynamically consistent picture, then, the normal state must deviate from the FL line and this is accomplished by turning on an excitation gap at  $T \leq T^*$ .

The dashed lines in Figs. 8(c) and 8(d) show a more reasonable extrapolated normal state (labeled PG) which is equivalent to the solid line for  $T \geq T_c$  and distinct for  $T < T_c$ . This extrapolation is taken to be consistent with the conservation of entropy,  $S = \int_0^T C_v/T dT$ , i.e., the shaded areas in (c) and (d). This construction for the  $T \leq T_c$  normal state is similar to the procedure followed experimentally,<sup>24</sup> and, in effect, removes phase-coherent contributions which enter via  $\Delta_{sc}$ . This construction is by no means unique; all that is required is that the entropy of the extrapolated normal and of the superconducting states be equal at  $T = T_c$ . As shown in the figure, we chose, for simplicity, a straight line extrapolation for  $C_v/T$ . Moreover, this choice is consistent with our expectation that there would be, in the “normal state,” a finite intercept for  $C_v/T$ .

Just as a gap is present above  $T_c$ , the underlying normal phase below  $T_c$  (labeled PG) is to be distinguished from the FL extrapolation; it also contains an excitation gap. Indeed, this is consistent with what has been claimed experimentally:<sup>24</sup> *a thermodynamically consistent picture of  $C_v$  reflects a gap in the  $T \leq T_c$  normal-state spectrum, not directly related to the condensate.* While Figs. 8(c) and 8(d) are similar to what is in the data in underdoped cuprates, in our analysis the “normal” state  $C_v/T$  and  $S$  are linear and

quadratic in  $T$ , respectively. Slightly different power laws have been assumed experimentally. A rough estimate of the condensation energy can be obtained from the integrated area between the solid line (for the superconducting state) and the dashed line (for the extrapolated normal state) in Fig. 8(d). It should also be noted that a more meaningful measure of the condensation energy is obtained by computing the magnetic-field-dependent Gibbs free energy. This is more complicated to implement both theoretically and experimentally.

## B. Comparison with vortex core and $C_v$ measurements

The presence of a pseudogap in the underlying normal state of the superconducting phase is also consistent with the observations by Renner and co-workers<sup>8</sup> based on STM measurements within a vortex core. While one might be concerned about magnetic field,  $H$ , effects in interpreting these data, it should be noted that  $H$  appears to have a rather weak effect<sup>49</sup> on pseudogap phenomena, as measured by  $T^*$  and  $\Delta(H)$ . (In more overdoped samples the field dependence becomes more apparent<sup>50</sup>.) By contrast  $T_c$  is more sensitive to  $H$ .

Indeed, this weak dependence on  $H$  is often invoked in the literature as strong evidence against the “preformed” pair scenario. In the usual BCS case, pairs form precisely when phase coherence sets in. However, in the case of a pseudogap superconductor where the coupling is stronger, pairs form above  $T_c$  without an underlying phase coherence. It is clear that a magnetic field lowers  $T_c$  by destroying phase coherence. However, “preformed” pairs will survive  $H$ , leaving the excitation gap in tact. Stated alternatively, a magnetic field (just like magnetic impurities) breaks time reversal symmetry, and therefore makes it energetically unfavorable to form Cooper pairs which are comprised of time-reversed single-particle states. In contrast, finite-momentum

pair excitations, which are responsible for the pseudogap in our approach, are not formed in time-reversed states, and as such, they are not as susceptible to external magnetic fields or to magnetic impurities. A more microscopic theory of the characteristic temperatures  $T^*(H)$  and  $T_c(H)$  at small  $H$  will be presented in a forthcoming paper. The field insensitivity of the former can be traced to the small size of the coherence length.<sup>51</sup>

In Fig. 9, we plot our results for the SIN tunneling characteristics,  $dI/dV$ , and the computed entropy and specific heat in a pseudogap superconductor, and compare with experiment.<sup>24,8,52</sup> To obtain the extrapolated normal state (called PG) in  $dI/dV$ , we set the superconducting order parameter  $\Delta_{sc}$  to zero, but maintain the total excitation gap to be same as in a phase coherent, superconducting state—with nonzero  $\Delta_{sc}$  (called SC). This procedure presumes that when the condensate is absent, the pseudogap  $\Delta_{pg}$  must correspond to the full excitation gap. Thus it should reflect the pairs which would otherwise be condensed. The characteristic behavior of  $dI/dV$  measured in an SIN configuration is presented as a comparison between theory (left) and experiment (right) in the upper panels of Fig. 9. Here the experimental curves are taken from Ref. 8, measured for underdoped Bi2212 inside (PG) and outside (SC) a vortex core, respectively. The non-Fermi-liquid nature of the extrapolated normal state can be clearly seen. In a similar fashion, we show the comparisons for the extrapolated entropy and specific heat between our theory and experiments of Ref. 24 for  $Y_{0.8}Ca_{0.2}Ba_2Cu_3O_{7-\delta}$ . Here  $\gamma = C_v/T$ . The agreement between the theoretically computed curves and experimentally deduced curves provides reasonable support for the present theoretical picture.

### C. Discussion

In this section we revisit some of the issues raised in this paper and in experiments on  $C_v$ , tunneling, vortex core, and related spectroscopies. In contrast to what has been presented up until now, here we are more qualitative and, in some instances, more speculative.

*Intrinsic tunneling experiments:*<sup>53</sup> Considerable attention has been directed towards intrinsic tunneling experiments (in stacked layers), not only because they yield different results from STM (Refs. 44 and 21) and from point contact/break junction<sup>45</sup> experiments, but also because they sometimes reveal an unexpected sharp feature (or second peak in  $dI/dV$ ) presumably associated with superconductivity. This peak occurs in addition to a broader excitation gap feature (which is more like that found in single-junction experiments) and it vanishes for  $T \geq T_c$ . There is, as yet, no complete convergence between different intrinsic Josephson junction (IJJ) tunneling experiments. On overdoped samples Suzuki and co-workers<sup>54</sup> have found anomalously sharp and large amplitude (second) peaks whose presence correlates with long-range order, while, by contrast, Latyshev and co-workers<sup>55</sup> find only a single maximum in  $dI/dV$  below  $T_c$ , which rather smoothly evolves into the normal state peak. However, for underdoped samples, Krasnov and co-workers<sup>53</sup> report two maxima below  $T_c$ , with a much less

pronounced sharp feature than in Ref. 54 (although the latter appears to be descended from the more anomalous features reported earlier by Suzuki *et al.*). Earlier work<sup>56</sup> by some of these same authors reported  $dI/dV$  characteristics in HgBr<sub>2</sub>-intercalated Bi2212 samples. In advantage, the Joule heating, which was considered to be a problem in experiments on IJJ at high bias current,<sup>54</sup> can therefore be significantly suppressed. These latter observations were more in line with those found by other groups<sup>45,8</sup> in single-junction experiments. In contrast to their more recent work,<sup>53</sup> in these intercalated samples the peak-dip-hump features were clearly visible at characteristic energies in the ratio 2:3:4.

There is in all these experiments the possibility that the so-called superconducting peak is an artifact of self-heating or other nonequilibrium effects, which would be present when there is a nonzero critical current. Its absence in single-junction experiments would, otherwise, be difficult to explain. These latter experiments correlate well with ARPES. Moreover, they also correlate with inferences from  $C_v$  and other bulk data.<sup>57,9</sup> We have no simple explanation for the sharp feature in tunneling. Within our approach there is a single excitation gap  $\Delta$  above as well as below  $T_c$ . Although the critical current<sup>16</sup>  $I_c$  reflects the order parameter  $\Delta_{sc}$ , which vanishes at  $T_c$ , this order parameter contribution is not expected to show up in quasiparticle tunneling as a second gap feature. Of these IJJ experiments, the data which seem not incompatible with our picture are those of Yurgens *et al.*<sup>56</sup> and, possibly, Latyshev *et al.*,<sup>55</sup> the latter authors, nevertheless, find much sharper maxima in  $dI/dV$  than we would have.

*Quantum critical points:* Both theorists<sup>58</sup> and experimentalists<sup>41,24</sup> have recently turned their attention to quantum critical phase transitions. Moreover, these phenomena are assumed to be related to pseudogap effects. Indeed, Loram and co-workers<sup>24</sup> presume that  $\Delta_{pg}$  (which, in their approach, is taken to be temperature independent) is proportional to  $T^*$ . Then at some critical doping concentration ( $x \approx 0.19$ ),  $\Delta_{pg}$  appears to vanish and they infer that  $T^* \rightarrow 0$ . By contrast, we find that  $\Delta_{pg}$  is more closely associated with  $(T^* - T_c)$ , which does not lead to a zero-temperature phase transition, even when  $\Delta_{pg}$  vanishes.

At low  $x$ , on the other hand, there may be something more dramatic like a first-order or quantum critical phase transition going on — at the superconductor-insulator boundary. Here the excitation gap is maximum on the one side of the boundary and yet the superconducting order parameter disappears on the other. (In the present picture this disappearance was found to arise from the localization of  $d$ -wave pairs<sup>15</sup>.) At low  $x$ , this superconductor-insulator transition also appears in the presence of a magnetic field<sup>59</sup> when the field is large enough to drive the system into the normal phase. It also appears with impurity pair breaking.<sup>60</sup> All three of these experiments may be interpreted as suggesting that the fermionic excitation gap  $\Delta$  survives in the presence of pair breaking (by large fields or impurities) or low hole concentrations—thereby leading to an insulating fermionic excitation spectrum. Some confirmation of this conjecture comes from NMR experiments<sup>49</sup> which seem to imply that  $\Delta$  does not vary with  $H$ , once the pseudogap is well estab-

lished. And the STM measurements,<sup>8</sup> in general, as well as inside a vortex core seem consistent with the observation that  $\Delta$  is only weakly  $H$  dependent. One cannot, of course, ignore Mott insulating effects at this superconductor-insulator boundary as well. However, whatever physical mechanism is dominant, the fact that the superconductor-insulator transition is a robust feature associated with the disappearance of superconductivity, whether by pair breaking or by doping, needs to be addressed.

*Incoherent contributions to the spectral function in photoemission:* Recent photoemission experiments<sup>61,30</sup> indicate that the relative weight of the coherent contribution to the spectral function decreases rapidly with decreasing  $x$ . Ignoring the incoherent term  $\Sigma_0$  in the self-energy (as we have here) will necessarily affect any quantitative inferences about the systematic  $x$  dependence of the spectral function and, thereby, of  $C_v$  or the related condensation energy. This term can only be put in by hand in the present approach; it arises here from diagrams other than the particle-particle terms which give rise to the superconductivity and pseudogap. Moreover, the measured systematic  $x$  dependence of the coherent spectral weight, which has been inferred from photoemission,<sup>61,30</sup> is likely to be consistent with the inferences based on thermodynamics<sup>24</sup> for the  $x$  dependence of the entropy  $S$  and related condensation energy. However, when the contribution from  $\Sigma_0$  is sizable, relative to the coherent terms, one cannot include it (by hand) without self-consistently also re-solving for the chemical potential  $\mu$  and, hence, also for  $\Delta$  and  $T_c$ , etc. This extensive numerical program would take us too far afield to implement here.

In addition, this  $\Sigma_0$  contribution is needed to arrive at the well-known<sup>62</sup> dip-hump features of photoemission. When this term is artificially added, we are able to obtain this latter structure which will scale with the excitation gap  $\Delta$ . Indeed, a dependence on  $\Delta$  is plausible since we presume that  $\Sigma_0$  is associated with various (electron-hole) polarizabilities, which in the superconducting and pseudogap states reflect the nonvanishing excitation gap. It is, however, essential (to obtain dip-hump features) that the imaginary part of  $\Sigma_0$  turn on rather abruptly at frequencies somewhere between  $\Delta$  and  $2\Delta$ . Indeed, the step function model introduced in Ref. 63 seems to accomplish this quite well, but we know of no simple microscopic mechanism which yields this rapid frequency onset.

## VI. CONCLUSIONS

This paper has raised some issues which have a number of important ramifications. We suggest that specific heat and vortex core experiments have provided strong evidence that the normal state underlying the superconducting phase is not a Fermi liquid. Thus BCS theory cannot be applied to the underdoped cuprates, without some modification. Since we have, as yet, very little alternative to BCS, it is natural first to try to extend it slightly. We believe the simplest and most benign modification is to adopt the Leggett extension of the ground-state wave function, Eq. (1) (which is applicable to weak and strong coupling  $g$ ), and extend his scheme to finite

$T$ . Within this approach we were able in the past to perform a number of concrete calculations,<sup>13–17</sup> and, in the present paper, explore the behavior somewhat above and below  $T_c$  of the specific heat  $C_v$  and quasiparticle tunneling characteristics  $dI/dV$ . This present study led us naturally to analyze the nature of superconducting phase coherence in the presence of a pseudogap.

Our study of  $C_v$  and  $dI/dV$  is based on a Green's function decoupling scheme chosen to be consistent with Eq. (1). The spectral functions which enter these two physical quantities depend, in turn, on the self-energy which is the sum of Eqs. (9) and (10), where throughout we have ignored the incoherent term  $\Sigma_0$ , which enters through diagrams other than those responsible for the superconducting and pseudogaps. It should be noted that this form for  $\Sigma$  is different from that introduced phenomenologically by Franz and Millis<sup>25</sup> and by Norman and Ding.<sup>63</sup> One of these groups,<sup>25</sup> in particular, emphasized the effects of the temperature-dependent scattering rate. Here, by contrast, we emphasize the effects of long-range phase coherence which sets in at  $T_c$ .

Because of the breakdown of BCS theory, in a superconductor with a pseudogap, the standard simplifications, such as Landau-Ginzburg expansions and Bogoliubov–de Gennes approaches,<sup>26</sup> are not expected to hold, at least without some modifications. For the BCS case, the expansion in terms of a small order parameter which is identical to the excitation gap at  $T_c$  is possible. However, when the order parameter and the excitation gap are distinct as in the pseudogap case, there is no straightforward way to expand the free energy in terms of a small order parameter and to reflect the existence of a well-established excitation gap simultaneously.

It should be emphasized, finally, that, in the non-BCS superconductor, there is an important distinction between  $T_c$  and the zero-temperature excitation gap  $\Delta(0)$ . In the strong-coupling, but still fermionic, regime, as the pseudogap increases,  $T_c$  is suppressed.<sup>4,5,15</sup> This observation allows us to respond to the widely repeated criticism of this “preformed” pair approach: namely, that<sup>49</sup> “the gap is not closely tied to the onset of superconductivity”—as inferred from, say, the lack of magnetic field dependence in the former. Here we claim that in contrast to BCS theory, the excitation gap  $\Delta$  is expected to be robust with respect to standard pair breaking perturbations (such as magnetic fields and impurity scattering), while the order parameter  $\Delta_{sc}$  is not. As emphasized throughout this paper, the distinction between these two quantities is an essential component of the “preformed” pair approach.

## ACKNOWLEDGMENTS

This work was supported by the NSF-MRSEC, No. DMR-9808595 (Q.C. and K.L.), and by the University of Illinois (I.K.). We thank A. V. Balatsky, K. E. Gray, Ying-Jer Kao, V. M. Krasnov, J. W. Loram, and J. F. Zasadzinski for helpful discussions.

- \*Present address: National High Magnetic Field Laboratory, 1800 East Paul Dirac Drive, Tallahassee, FL 32310.
- <sup>1</sup>P. A. Lee and X.-G. Wen, Phys. Rev. Lett. **78**, 4111 (1997).
  - <sup>2</sup>P. W. Anderson, *The Theory of Superconductivity in the High- $T_c$  Cuprates* (Princeton University Press, Princeton, NJ, 1997).
  - <sup>3</sup>B. Jankó, J. Maly, and K. Levin, Phys. Rev. B **56**, R11 407 (1997).
  - <sup>4</sup>J. Maly, B. Jankó, and K. Levin, Physica C **321**, 113 (1999).
  - <sup>5</sup>J. Maly, B. Jankó, and K. Levin, Phys. Rev. B **59**, 1354 (1999).
  - <sup>6</sup>A. Junod, A. Erb, and Ch. Renner, Physica C **317-318**, 333 (1999).
  - <sup>7</sup>Y. J. Uemura, Physica C **282-287**, 194 (1997).
  - <sup>8</sup>Ch. Renner, B. Revaz, K. Kadowaki, I. Maggio-Aprile, and Ø. Fischer, Phys. Rev. Lett. **80**, 3606 (1998).
  - <sup>9</sup>T. Timusk and B. Statt, Rep. Prog. Phys. **62**, 61 (1999).
  - <sup>10</sup>G. Deutscher, Nature (London) **397**, 410 (1999).
  - <sup>11</sup>M. Randeria, in *Bose Einstein Condensation*, edited by A. Griffin, D. Snoke, and S. Stringari (Cambridge University Press, Cambridge, UK, 1995), pp. 355–392.
  - <sup>12</sup>P. Nozières and S. Schmitt-Rink, J. Low Temp. Phys. **59**, 195 (1985).
  - <sup>13</sup>I. Kosztin, Q. J. Chen, B. Jankó, and K. Levin, Phys. Rev. B **58**, R5936 (1998).
  - <sup>14</sup>I. Kosztin, Q. J. Chen, Y.-J. Kao, and K. Levin, Phys. Rev. B **61**, 11 662 (2000).
  - <sup>15</sup>Q. J. Chen, I. Kosztin, B. Jankó, and K. Levin, Phys. Rev. B **59**, 7083 (1999).
  - <sup>16</sup>Q. J. Chen, I. Kosztin, B. Jankó, and K. Levin, Phys. Rev. Lett. **81**, 4708 (1998).
  - <sup>17</sup>Q. J. Chen, I. Kosztin, and K. Levin, Phys. Rev. Lett. **85**, 2801 (2000).
  - <sup>18</sup>A. J. Leggett, in *Modern Trends in the Theory of Condensed Matter*, edited by A. Pekalski and J. Przystawa (Springer-Verlag, Berlin, 1980), pp. 13–27.
  - <sup>19</sup>H. Ding, T. Yokoya, J. C. Compuzano, T. Takahashi, M. Randeria, M. R. Norman, T. Mochiku, K. Hadowaki, and J. Giapintzakis, Nature (London) **382**, 51 (1996).
  - <sup>20</sup>A. G. Loeser, Z.-X. Shen, D. S. Dessau, D. S. Marshall, C. H. Park, P. Fournier, and A. Kapitulni, Science **273**, 325 (1996).
  - <sup>21</sup>S. H. Pan, E. W. Hudson, A. K. Gupta, K.-W. Ng, H. Eisaki, S. Uchida, and J. C. Davis, Phys. Rev. Lett. **85**, 1536 (2000).
  - <sup>22</sup>J. W. Loram, K. A. Mirza, J. R. Cooper, W. Y. Liang, and J. M. Wade, J. Supercond. **7**, 243 (1994).
  - <sup>23</sup>J. W. Loram, K. A. Mirza, J. R. Cooper, A. Athanassopoulou, and W. Y. Liang, in *Proceedings of the 10th Annual HTS Workshop*, edited by B. Batlogg *et al.* (World Scientific, Singapore, 1996), pp. 341–344.
  - <sup>24</sup>J. W. Loram, K. A. Mirza, J. R. Cooper, and J. L. Tallon, J. Phys. Chem. Solids **59**, 2091 (1998).
  - <sup>25</sup>M. Franz and A. J. Millis, Phys. Rev. B **58**, 14 572 (1998).
  - <sup>26</sup>M. Franz and Z. Tesanovic, Phys. Rev. B **63**, 064516 (2001).
  - <sup>27</sup>P. A. Lee and X.-G. Wen, cond-mat/0008419, Phys. Rev. B (to be published).
  - <sup>28</sup>V. J. Emery and S. A. Kivelson, Nature (London) **374**, 434 (1995).
  - <sup>29</sup>We make a distinction here between tunneling and ARPES in the presence of an isotropic tunneling matrix element. For more directional tunneling, the difference between ARPES and tunneling experiments may be less apparent.
  - <sup>30</sup>D. L. Feng, D. H. Lu, K. M. Shen, C. Kim, H. Eisaki, A. Damascelli, R. Yoshizaki, J.-I. Shimoyama, K. Kishio, G. D. Gu, S. Oh, A. Andrus, J. O'Donnell, J. H. Eckstein, and Z.-X. Shen, Science **289**, 277 (2000).
  - <sup>31</sup>L. P. Kadanoff and P. C. Martin, Phys. Rev. **124**, 670 (1961).
  - <sup>32</sup>It should be noted, however, that Eq. (3) is not derived diagrammatically from Fig. 1. Instead, it was derived by truncating the equations of motion at the three-particle level ( $G_3$ ) and factorizing  $G_3$  into one- and two-particle Green's functions (Ref. 31). In this way, the pair susceptibility contains one bare and one dressed fermion line. This is in the same spirit as the derivation of the Gor'kov equation. Figure 1 is a representation of the resulting equations for the self-energy and the  $T$  matrix.
  - <sup>33</sup>A.-M. Daré, Y. M. Vilks, and A.-M. S. Tremblay, Phys. Rev. B **53**, 14 236 (1996).
  - <sup>34</sup>For the  $d$ -wave case, we have also studied the effects associated with introducing a  $\mathbf{k}$  dependence in  $\gamma$ , and found that these effects are negligible.
  - <sup>35</sup>A. L. Fetter and J. D. Walecka, *Quantum Theory of Many-Particle Systems* (McGraw-Hill, San Francisco, 1971).
  - <sup>36</sup>Here by  $dN(\omega)/dT$ , we mean the Fermi-function-weighted average over a broad range of frequency. See the third term in Eq. (17).
  - <sup>37</sup>It should be emphasized that the temperature dependence of  $C_v$  at  $T \gtrsim T_c$  is dominated by  $dN(\omega)/dT$ , instead of  $N(\omega)$  itself. In fact the contributions of these two functions are in opposite directions as a function of temperature. This observation implies that one cannot extract the size of the excitation gap from the specific heat without taking proper account of the  $T$  dependence of the density of states. It should also be noted that the curvature above but in the vicinity of  $T_c$  also reflects the subtle feature at  $T_c$  which appears in the excitation gap.
  - <sup>38</sup>H. Ding, M. R. Norman, T. Yokoya, T. Takeuchi, M. Randeria, J. C. Campuzano, T. Takahashi, T. Mochiku, and K. Kadowaki, Phys. Rev. Lett. **78**, 2628 (1997).
  - <sup>39</sup>For this choice of  $t'$ , the van Hove singularities appear inside the filled lower half band. Because these effects were not particularly relevant in our previous studies, this complication was ignored previously.
  - <sup>40</sup>A. Hosseini, R. Harris, S. Kamal, P. Dosanjh, J. Preston, R.-X. Liang, W. N. Hardy, and D. A. Bonn, Phys. Rev. B **60**, 1349 (1999).
  - <sup>41</sup>T. Valla, A. V. Fedorov, P. D. Johnson, B. O. Wells, S. L. Hulbert, Q. Li, G. D. Gu, and N. Koshizuka, Science **285**, 2110 (1999).
  - <sup>42</sup>Since the pseudogap equation (6) indicates  $\Delta_{pg}^2 \propto T^{3/2}$  at low  $T$ , and  $\Delta_{pg}^2$  is roughly linear in  $T$  at  $T \lesssim T_c$ , this choice of  $\gamma \propto T^3$  below  $T_c$  will give rise to a temperature dependence of the effective quasiparticle peak width  $\gamma' \propto T^\alpha$  with  $\alpha = 4 \sim 4.5$  for  $T \lesssim T_c$ , via Eq. (13). This is consistent with the experimentally observed  $T^4 \sim T^5$  dependence of the quasiparticle scattering rate (Ref. 40). Above  $T_c$ , the  $T$  dependence of  $\Delta_{pg}$  is weak, so that  $\gamma' \propto T$ , in agreement with ARPES data (Ref. 41).
  - <sup>43</sup>G. D. Mahan, *Many-Particle Physics*, 2nd ed. (Plenum Press, New York, 1990).
  - <sup>44</sup>Ch. Renner, B. Revaz, J. Y. Genoud, K. Kadowaki, and Ø. Fischer, Phys. Rev. Lett. **80**, 149 (1998).
  - <sup>45</sup>N. Miyakawa, P. Guptasarma, J. F. Zasadzinski, D. G. Hinks, and K. E. Gray, Phys. Rev. Lett. **80**, 157 (1998); N. Miyakawa, J. F.

- Zasadzinski, L. Ozyuzer, P. Guptasarma, D. G. Hinks, C. Kendziora, and K. E. Gray, *ibid.* **83**, 1018 (1999).
- <sup>46</sup>E. Demler and S.-C. Zhang, *Nature (London)* **396**, 733 (1998).
- <sup>47</sup>M. R. Norman, M. Randeria, B. Jankó, and J. C. Campuzano, *Phys. Rev. B* **61**, 14 742 (2000).
- <sup>48</sup>A. J. Leggett, *J. Phys. Chem. Solids* **49**, 1729 (1998).
- <sup>49</sup>K. Gorny, O. M. Vyaselev, J. A. Martindale, V. A. Nandor, C. H. Pennington, P. C. Hammel, W. L. Hults, J. L. Smith, P. L. Kuhns, A. P. Reyes, and W. G. Moulton, *Phys. Rev. Lett.* **82**, 177 (1999).
- <sup>50</sup>G. Zheng, H. Ozaki, W. Clark, Y. Kitaoka, P. Kuhns, A. Reyes, W. Moulton, T. Kondo, Y. Shimakawa, and Y. Kubo, *Phys. Rev. Lett.* **85**, 405 (2000).
- <sup>51</sup>Y. Yanase and K. Yamada, *J. Phys. Soc. Jpn.* **69**, 2209 (2000).
- <sup>52</sup>In what follows we ignore the contribution from bound states to the core tunneling spectroscopy. Understanding these bound states will require a generalization of Bogoliubov–de Gennes theory for our extended BCS approach.
- <sup>53</sup>V. M. Krasnov, A. Yurgens, D. Winkler, P. Delsing, and T. Claesson, *Phys. Rev. Lett.* **84**, 5860 (2000).
- <sup>54</sup>M. Suzuki, T. Watanabe, and A. Matsuda, *Phys. Rev. Lett.* **82**, 5361 (1999).
- <sup>55</sup>Y. Latyshev, V. Pavlenko, S.-J. Kim, L. N. Bulaevskii, M. J. Graf, A. V. Balatsky, N. Morozov, and M. P. Maley, *Physica C* **341-348**, 1499 (2000).
- <sup>56</sup>A. Yurgens, D. Winkler, T. Claesson, S.-J. Hwang, and J.-H. Choy, *Int. J. Mod. Phys. B* **13**, 3758 (1999).
- <sup>57</sup>J. L. Tallon and J. W. Loram, *Physica C* **349**, 53 (2001).
- <sup>58</sup>S. Chakravarty, R. B. Laughlin, D. K. Morr, and C. Nayak, *Phys. Rev. B* **63**, 094503 (2001).
- <sup>59</sup>Y. Ando, G. S. Boebinger, A. Passner, T. Kimura, and K. Kishio, *Phys. Rev. Lett.* **75**, 4662 (1995).
- <sup>60</sup>Y. Zhao, H. K. Liu, G. Yang, and S. X. Dou, *J. Phys.: Condens. Matter* **5**, 3623 (1993).
- <sup>61</sup>H. Ding, J. R. Engelbrecht, A. Wang, J. C. Campuzano, S.-C. Wang, H.-B. Yang, R. Rogan, T. Takahashi, K. Kadowaki, and D. C. Hinks, cond-mat/0006143 (unpublished).
- <sup>62</sup>M. R. Norman, H. Ding, H. Fretwell, M. Randeria, and J. C. Campuzano, *Phys. Rev. B* **60**, 7585 (1999).
- <sup>63</sup>M. R. Norman and H. Ding, *Phys. Rev. B* **57**, 11 089 (1998).